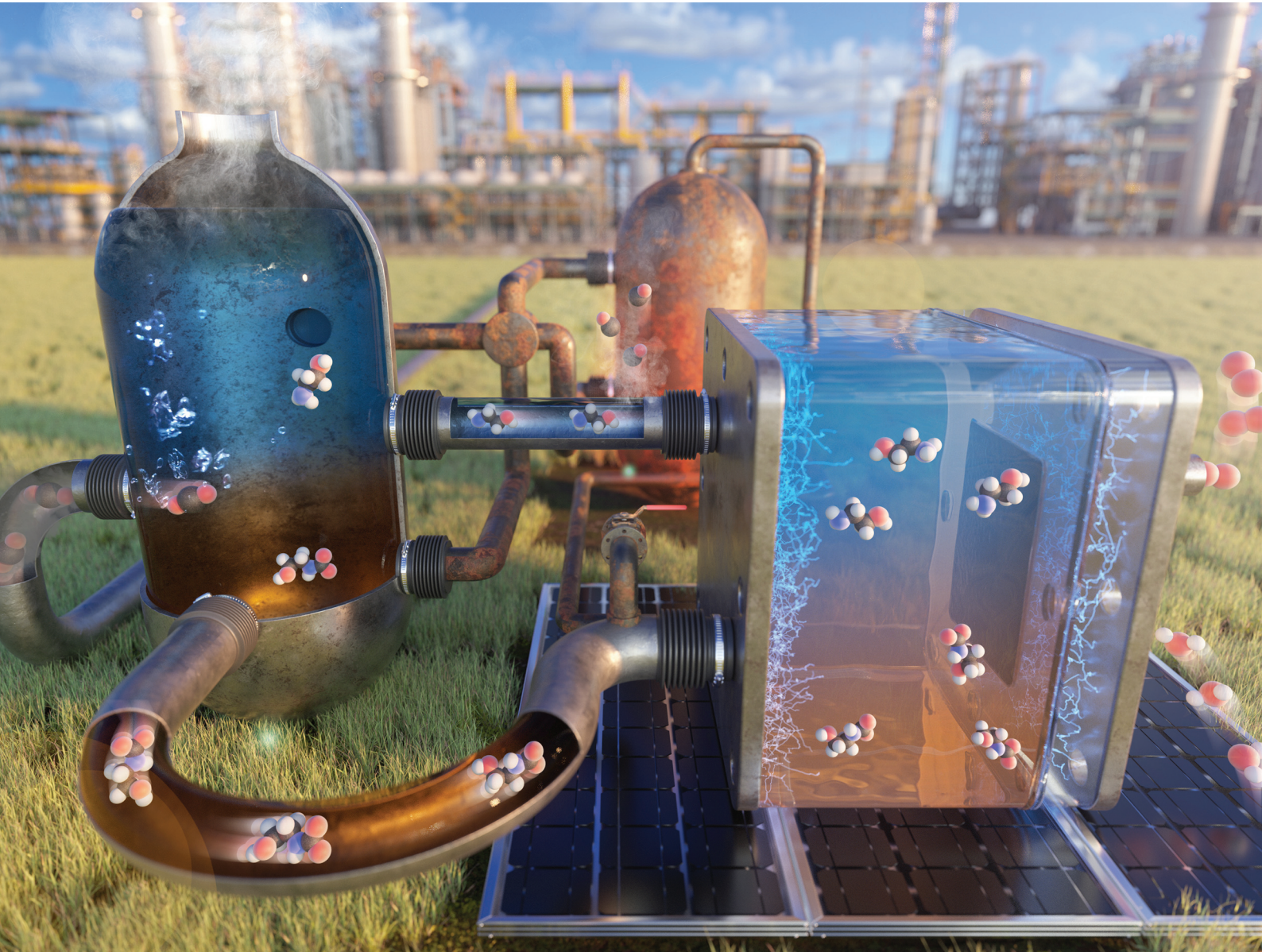


Green Chemistry

Cutting-edge research for a greener sustainable future

rsc.li/greenchem



ISSN 1463-9262

PAPER

Yun Jeong Hwang, Jonggeol Na *et al.*
Techno-economic analysis and life-cycle assessment of the
electrochemical conversion process with captured CO₂ in an
amine-based solvent



Cite this: *Green Chem.*, 2023, **25**, 10398

Techno-economic analysis and life-cycle assessment of the electrochemical conversion process with captured CO₂ in an amine-based solvent†

Suhyun Lee, ^{a,b} Woong Choi, ^{c,d} Jae Hyung Kim, ^e Sohyeon Park, ^a Yun Jeong Hwang ^{f,g} and Jonggeol Na ^{a,b}

The direct electrochemical conversion of captured CO₂ technology has received global attention as an alternative to the current energy-demanding amine solvent regeneration and separation processes of the conventional carbon capture process; however, the identification of the potential advantages of this process from both the economic and environmental perspectives is not straightforward. Here, we present process designs of two commercial-scale carbon capture and utilization (CCU) processes: a direct electrochemical conversion process *via* the captured CO₂ reduction reaction (cCO₂RR) in a monoethanolamine (MEA)-based medium and an electrochemical conversion process *via* the CO₂ reduction reaction (CO₂RR) in aqueous electrolyte media. As a result of the techno-economic analysis, the leveled cost of product CO (LCOC) of the cCO₂RR process, which reflects the current technology level, is 3.5 times higher than that of the CO₂RR process, resulting in low economic feasibility. However, if the technology of cCO₂RR develops to the same level as that of the CO₂RR, the LCOC can be 6.1% lower than that of the CO₂RR process, which shows that the cCO₂RR technology has good economic potential. Furthermore, the life cycle assessment revealed that when using renewable electricity, the cCO₂RR process can have a much more positive environmental impact than CO₂RR, even at the current technological performance level. We highlighted that the analysis of the proposed cCO₂RR technology will become a good guideline for the development of an integrated and new type of CCU technology without being complacent with the current CCU technology.

Received 29th June 2023,
 Accepted 5th September 2023
 DOI: 10.1039/d3gc02329j
rsc.li/greenchem

Introduction

Carbon capture and utilization (CCU) technology has attracted significant attention as an anthropogenic carbon recycling

^aDepartment of Chemical Engineering and Materials Science, Ewha Womans University, Seoul 03760, Republic of Korea. E-mail: jgna@ewha.ac.kr

^bGraduate Program in System Health Science and Engineering, Ewha Womans University, Seoul 03760, Republic of Korea

^cEnergy Storage and Distributed Resources Division, Lawrence Berkeley National Laboratory, Berkeley, California 94720, USA

^dClean Energy Research Center, Korea Institute of Science and Technology (KIST), Seoul 02792, Republic of Korea

^eClean Fuel Research Laboratory, Korea Institute of Energy Research, 152 Gajeong-ro, Yuseong-gu, Daejeon 34129, Republic of Korea

^fDepartment of Chemistry, Seoul National University, Seoul 08826, Republic of Korea. E-mail: yjhwang1@snu.ac.kr

^gCenter for Nanoparticle Research, Institute for Basic Science (IBS), Seoul 08826, Republic of Korea

† Electronic supplementary information (ESI) available. See DOI: <https://doi.org/10.1039/d3gc02329j>

‡ These authors contributed equally to this work.

strategy to realize a carbon-neutral society.¹ To date, carbon capture and carbon utilization technologies have been developed independently, but both capital and operating costs have hindered their commercialization.^{2,3} Amine-based chemicals, particularly monoethanolamine (MEA), have been commercially used as carbon-capturing media at the point sources (*e.g.*, power plants, cement production, and petrochemical facilities) due to their affordability and fast CO₂ capture kinetics.^{4,5} However, the regeneration of CO₂ from MEA requires a high temperature and a large amount of thermal energy due to the trapping of CO₂ as a carbamate (which is thermodynamically stable) by the amine group of MEA.⁶ This energy-demanding CO₂ stripping unit process makes the entire carbon capture process expensive and environmentally toxic.

For CO₂ capture, various attempts have been made to develop amine solvents with a lower regeneration energy, while maintaining high capture performances (*e.g.*, 2-amino-2-methyl-1-propanol, diethanolamine, methyldiethanolamine, triethanolamine, and amine-based blends).^{7–11} The use of

alternative solvents, such as sterically-hindered amines weakening C–N bonding in carbamate or tertiary amines forming bicarbonate due to a lack of replaceable proton, can reduce the regeneration energy by up to 10–30% compared to MEA with the same total amine mass concentration.¹² Nevertheless, the weaker CO₂ binding inevitably leads to a lower CO₂ capture rate resulting in inferior total capture cost. Second, in terms of carbon utilization, the electrochemical CO₂ reduction reaction (CO₂RR) technology that captures CO₂ and supplies it in the pure gas form to a CO₂ electrolyzer is attracting attention as a sustainable technology in that it can utilize renewable energy. However, the low-price competitiveness of the products of the CCU technology compared to petroleum-based chemicals has hindered the application of the CCU technology.¹³ To generate high-purity CO₂, additional compression and purification processes are required after the CO₂ capture, which further increases the cost of the entire CCU process.¹⁴ Recent studies have proposed alternative systems to CO₂ stripping technologies for achieving significantly more cost-effective carbon CCU processes, such as the direct utilization technology of low-concentration CO₂ in flue gas.^{15,16} However, the conversion efficiency of these new systems is still rather low, and there are technical barriers, such as competition with the oxygen reduction reaction (ORR), toxic impurity poisoning, and poor electrochemical CO₂ reduction reaction (CO₂RR) performances.^{15,16}

Recently, integrated CCU systems, which perform a direct electrochemical conversion process *via* the captured CO₂ reduction reaction (cCO₂RR) utilizing various capture agents such as amine-based solutions, carbonate and bicarbonate solutions, ionic liquids and covalent organic frameworks, have emerged as an effective means to address the drawbacks of carbon capture and carbon utilization processes.^{2,17–23} The cCO₂RR process can save energy by excluding the capture media regeneration step that requires excessive thermal energy, and compression and product purification steps, which require electrical energy. Of course, a large amount of electrical energy ranging from 643 kJ mol_{CO₂}⁻¹ to 2412 kJ mol_{CO₂}⁻¹ can be consumed in the electrolysis step depending on the performance of the CO₂ to CO electrolysis process,¹⁴ but the impact of energy savings by excluding regeneration, compression and purification steps on improving the economics of the cCO₂RR cannot be ignored. In fact, Li *et al.* found that amine media based integrated processes can have an overall energy benefit of up to 44% compared to the conventional CO₂RR CCU technology.¹⁴ In amine based cCO₂RR systems, carbamate, rather than pure CO₂, is supplied to the electrochemical cells. Although the strong C–N binding affects the utilization of captured CO₂ in carbamate, studies have reported that a meaningfully high faradaic efficiency (FE; 72%) and current density (50 mA cm⁻²) can be achieved by employing cation-containing electrolytes.¹⁷ We have surveyed and summarized previous publications on the performances of the cCO₂RR technology in Table 1. However, the economic and environmental advantages of the commercial-scale cCO₂RR process are not straightforward. Previous studies^{11,14} that ana-

Table 1 Summary of cCO₂RR performances based on various previously reported catalysts

#	Catalyst	Capturing material	Additives	Cell type	Cell temp (°C)	FE	CO	HCOO ⁻	CH ₄	Voltage	Total current density (mA cm ⁻²)	Membrane	Ref.
1	Ag	1 M K ₂ CO ₃	—	MEA cell	rt	25	—	—	—	3.5 V (cell voltage)	150	BPM	38
2	Ag	3 M TBA ^a	—	MEA cell	rt	30	—	—	—	4 V (cell voltage)	200	BPM	11
3	Ag	3 M KHCO ₃	—	MEA cell	rt	81	—	—	—	—	—	BPM	39
4	Bi	3 M KHCO ₃	—	MEA cell	rt	—	64	—	—	4 V (cell voltage)	25	BPM	40
5	Cu foam	3 mM CTAB	—	MEA cell	rt	—	—	—	—	7.2 V (cell voltage)	100	BPM	41
6	Ag	2 M KCl	—	Flow cell	60	72	—	—	—	0.8 V (vs. RHE)	400	PEM (Nafion 117)	17
7	Ni–NC	5 M MEA	—	MEA cell	40	64.9	—	—	—	—	50	BPM	20
8	Porous In film	5 M MEA	0.1% CTAB	H-cell	rt	22.8	54.5	—	—	−0.8 V (vs. RHE)	—	Porous glass frit	4
9	Porous Pb film	5 M MEA	0.1% CTAB	H-cell	rt	2.9	60.8	—	—	−0.8 V (vs. RHE)	—	Porous glass frit	4
10	Porous Ag film	5 M MEA	0.1% CTAB	H-cell	rt	38.2	2.4	—	—	−0.8 V (vs. RHE)	—	Porous glass frit	4
11	Pb	1 M AMP ^b	0.7 M TEAC ^c in PC ^d	H-cell	75	—	45	—	—	−2.5 V (vs. Ag/AgCl)	25	PEM (Nafion 117)	19

^a Triethanolamine. ^b 2-Amino-2-methyl-1-propanol. ^c Tetraethylammonium chloride. ^d Propylene carbonate.

lyzed the economics and energy efficiency of the cCO₂RR process did not consider the commercial-scale carbon capture process or were limited to presenting new solvents other than the commercially used solvent MEA.²⁴

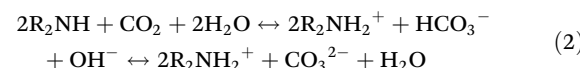
Herein, we present a rigorous techno-economic analysis and broad-range life cycle assessment (LCA) by considering a commercial-scale power plant, MEA solvent-based post-combustion capture (PCC) plant, and an electrochemical conversion process. In order to analyze the economic feasibility of the cCO₂RR and CO₂RR processes more objectively, both the actual current technology level and the optimistic future level of each process were analyzed. In particular, the CO₂ capture cost and levelized cost of product CO (LCOC) of the CO₂RR and cCO₂RR processes were derived and compared as an economic index, and sensitivity analysis related to the performances of electrochemical conversion, such as overpotential, FE, and current density, was performed.

Electrochemical captured CO₂ conversion

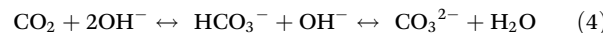
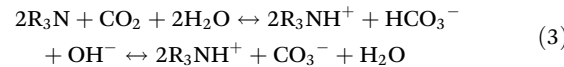
The CO₂RR has been considered one of the most active strategies for the conversion of CO₂ into valuable chemicals using electrical energy obtained from renewable energy sources. However, as the CO₂RR generally utilizes ultra-high purity (99.999%) CO₂ gas,^{25,26} the captured CO₂ must be subjected to additional CO₂ regeneration, purification, and compression steps (Fig. 1a). The cCO₂RR refers to the direct electrochemical reduction of captured CO₂ instead of pure CO₂ gas without additional energy-demanding steps (Fig. 1b). To compare cCO₂RR technologies with CO₂RR technologies, we surveyed and listed the previous publications on the performances of gaseous CO₂ reduction reactions into CO (Table 2). Also, the

energy diagram for better visualization to understand the difference between gaseous CO₂ and carbamate reduction reactions is given in Fig. S1 in the ESI.†

To understand the cCO₂RR, it is crucial to understand both CO₂ capture and reduction processes. The CO₂ capture process follows the acid–base reaction between CO₂ and bases. Briefly, primary and secondary amines, which are general CO₂ capturing materials, combine with CO₂ to produce carbamate–ammonium as conjugation acid–base pairs (eqn (1)), while also forming (bi)carbonate ions (eqn (2)). The distribution of carbamates and (bi)carbonates is determined by the pK_a values of amine-based CO₂ capturing materials.²⁷



The CO₂ capture kinetics in amine-based materials is governed by the strength of the newly formed C–N bonding in carbamates. The electron-donating and less steric-hindered R group provides a stronger C–N bonding.^{28,29} MEA, which is a primary amine with an electron-donating ethanol group, has been widely employed as a CO₂ capturing material because of its fast CO₂ capture kinetics, which is attributed to its stronger C–N bonding. Hydroxide solutions and tertiary amines capture CO₂ gas as (bi)carbonate ions (eqn (3) and (4)).



When compared to carbamates, these (bi)carbonates exhibit weaker CO₂ binding and slower CO₂ absorption.^{30,31} The CO₂ binding strength, which depends on the capturing

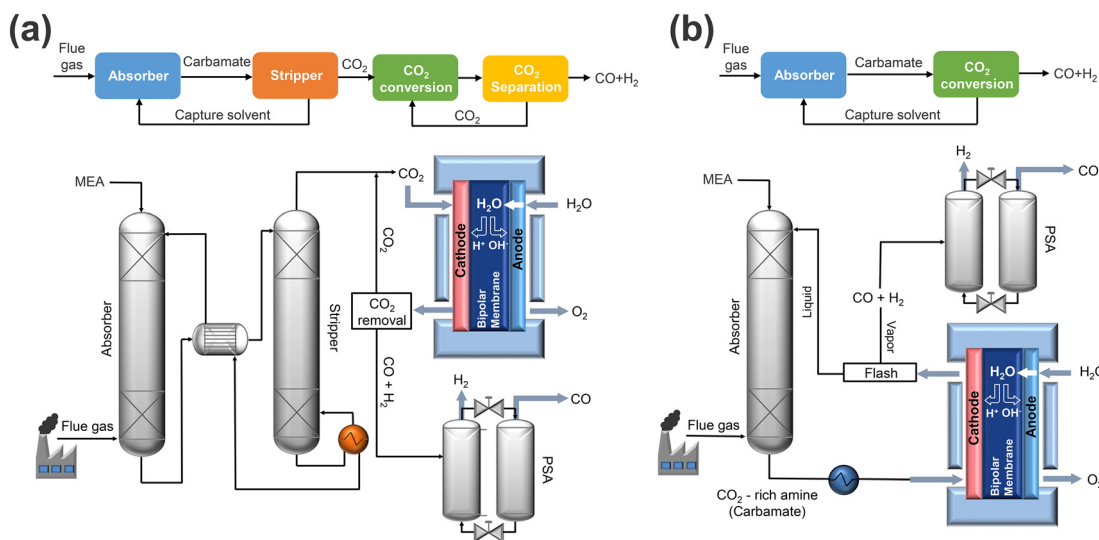


Fig. 1 Block diagrams and schematic representation of two possible routes for CO₂ capture and conversion technology. (a) CO₂ reduction reaction (CO₂RR) process and (b) captured CO₂ reduction reaction (cCO₂RR) process.

Table 2 Summary of CO₂RR performances based on various previously reported catalysts

#	Catalyst	Electrolyte	Cell type	Cell temp (°C)	FE _{CO}	Voltage	Total current (mA cm ⁻²)	Membrane	Ref.
1	Ag NPs	0.1 M CsOH	MEA	60	80	3.2 V (cell voltage)	630	AEM (PiperION)	42
2	Ag NPs	0.1 M KHCO ₃	MEA	60	60	3.2 V (cell voltage)	603	AEM (HQPC-tmIM)	43
3	Au/C	0.1 M KHCO ₃	MEA	60	85	3.0 V (cell voltage)	500	AEM (QAPPT)	44
4	Ag NPs	1 M CSHCO ₃	MEA	60	90	3.2 V (cell voltage)	420	AEM (PiperION)	45
5	O ₂ plasma treated Ag	0.01 M CsOH	MEA	rt	80	4 V (cell voltage)	500	AEM (QAPPT)	46
6	Ag/MPL-3C	0.1 M KHCO ₃	MEA	rt	96	3.78 V (cell voltage)	400	AEM (Sustainion)	47
7	Coral Ag	0.5 M KHCO ₃	MEA	rt	90	-0.79 V (vs. RHE)	312	AEM (Sustainion)	48
8	Ag NPs	1 M KOH	MEA	rt	95	3.0 V (cell voltage)	300	AEM (Sustainion)	49
9	Porous Ag	0.1 M KHCO ₃	MEA	rt	95	3.3 V (cell voltage)	200	AEM (Sustainion)	50
10	Ag	1 M KOH	MEA	rt	96	2.8 V (cell voltage)	192	AEM (AEMION)	51
11	3D AuAg	1 M KHCO ₃	MEA	rt	93	3.7 V (cell voltage)	186	AEM (Fumasep)	52
12	AuAg NPs	0.1 M KHCO ₃	MEA	rt	88	2.75 V (cell voltage)	95	AEM (Sustainion)	53
13	Ni-SA-NCs	0.5 M KHCO ₃	MEA	rt	99	2.76 V (cell voltage)	382	AEM (Sustainion)	54
14	Ni-N/C	0.1 M KHCO ₃	MEA	rt	~100	3.0 V (cell voltage)	299	AEM (Sustainion)	15
15	Ni-NG	0.1 M KHCO ₃	MEA	rt	90	2.78 V (cell voltage)	50	AEM (PSMIM)	46

materials, exhibits a tradeoff between CO₂ capture and regeneration. MEA, which exhibits a strong CO₂ binding strength, exhibits fast CO₂ capture kinetics and capacity,^{4,5} however, a large amount of energy is required to regenerate CO₂ from carbamates.⁶ In addition, although CO₂ regeneration from (bi)carbonate ions consumes less energy, it exhibits sluggish CO₂ capture kinetics and capacity.^{9,32}

In the cCO₂RR, the activation of the captured CO₂ is a key factor to initiate the CO₂ reduction reaction on the electrocatalyst surface, and thus CO₂ binding with the capturing material is required to be weakened. The reduction of (bi)carbonates with a weaker CO₂ binding strength exhibits a high FE and current density for the cCO₂RR. MEA is economically more favorable because of its faster CO₂ capture kinetics, efficiency, and capacity in terms of CO₂ capture.³² Meanwhile, the reduction of carbamates is expected to be more difficult due to the stronger CO₂ binding by C–N bonding. Therefore, to reduce carbamates efficiently, C–N bonding is required to be weakened by a catalytic atmosphere in the electrolyte. Although the catalytic performances of the cCO₂RR can be enhanced by increasing the reaction temperature,^{17,20} additional consumption of thermal energy has the similar drawback of sequential CO₂ capture and the CO₂RR. At the same time, increasing the reaction temperature can activate the competitive hydrogen evolution reaction (HER) more and rather decrease the faradaic efficiency for the CO₂ reduction. Proton-rich conditions can shift the chemical equilibrium and result in weakening of C–N bonding. Studies have reported that compared to an anion exchange membrane, which is generally used in the CO₂RR, a bipolar membrane (BPM) and a proton exchange membrane (PEM), which provide protons to the cathode, can be used to achieve higher *in situ* CO₂ (i-CO₂) regeneration and thus increased cCO₂RR performances.^{33–35} In addition, alkali-metal cations with a smaller effective size than ethanolammonium can facilitate the cCO₂RR, and the thinner electrochemical double layer (EDL) is proposed to assist a faster electron transfer to carbamates.^{17,36} The presence of the alkali-metal cation in the EDL is also demonstrated to modu-

late the activity and selectivity for the CO₂RR as well as the HER by affecting the charge density and interacting with the intermediate species. By the combination of these approaches, carbamate reduction has achieved a similar current density and FE to (bi)carbonate reduction (Table 1). As the cCO₂RR through carbamates requires a lower cost and exhibits the same catalytic performances due to the low CO₂ capture cost, in this study, we focused on the electrochemical reduction of carbamates as the cCO₂RR.

Currently, the products from the cCO₂RR are mostly limited to C1 products such as CO, formate, and methane. Therefore, Au, Ag, and single atom catalysts (SACs) have been demonstrated to produce two-electron transferred chemical CO, or oxophilic metals such as Bi and In are often used to produce formate from the cCO₂RR. The trend of the major products is similar between the cCO₂RR and conventional electrochemical CO₂ reduction reaction, which implies that the reaction paths are similar after CO₂ reduction is initiated on the catalyst surface. An additional purification process from an amine-based solution has to be designed for formate production, which varies the evaluation of the technology. In this study, we focused on CO production from the cCO₂RR, because of the high market demands of CO as syngas in the chemical industry.³⁷

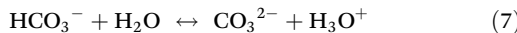
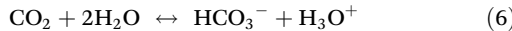
Assessment framework

Process description and modeling

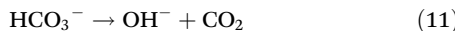
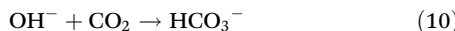
In this study, we designed the cCO₂RR and CO₂RR processes based on PCC technologies that capture 90% of the CO₂ from flue gas discharged from the process by referring to the information of an actual existing subcritical pulverized coal-fired power plant.⁵⁵ The composition and conditions of the flue gas used are summarized in Table S1 in the ESI.† Note that the key difference between the two processes is the existence of a stripper column. The CO₂RR process involves the following steps: absorption of CO₂ in an amine solvent, desorption of captured

CO_2 from the solvent at the stripper, utilization of purified CO_2 , removal of unreacted CO_2 from gas products, and the pressure swing adsorption (PSA) unit. For the c CO_2 RR, CO_2 conversion and MEA regeneration can be simultaneously conducted in the c CO_2 RR electrolyzer, thus removing the need for the stripper (Fig. 1). Specifically, the captured CO_2 (carbamate) is used directly as a reactant and electrochemically converted to CO. In addition, unreacted CO_2 in the c CO_2 RR combines with the MEA solvent to form a carbamate, and is not released together with the gas products of the electrolyzer.^{11,14} Consequently, no additional CO_2 removal from CO and H_2 products is required, thus further reducing the energy requirement of the c CO_2 RR. To systematically understand the CO_2 RR and c CO_2 RR process design, the process flow diagram (PFD) for each process is presented in Fig. S2, ESI.†

In the CO_2 capture process, the flue gas injected into the absorber makes contact with the MEA. Subsequently, the CO_2 of the flue gas is removed through the chemical reaction of the absorber. A rich amine stream, which means enriched CO_2 solution, is injected into the stripper that separates the captured CO_2 from the solvent to produce high purity CO_2 , followed by MEA regeneration. As CO_2 regeneration proceeds at a high temperature and requires a large amount of thermal energy, a preheating step is required to reduce heat energy at the reboiler of the stripper. For process efficiency, it was designed through heat exchange with the high-temperature stream discharged to the bottom of the stripper. However, in the c CO_2 RR process, as the reaction that occurs in the electrolyzer proceeds under mild operating conditions, such as room temperature, it is unnecessary to increase the temperature of the rich amine stream. Instead, the 59 °C carbamate solution discharged to the bottom of the absorber goes through a process of cooling down to room temperature. The reactions of both the absorber in the two CCU processes and the stripper in the CO_2 RR are presented in the equations below (eqn (5)–(13)). First, the equilibrium reactions for the solution chemistry of CO_2 absorption in an aqueous amine-based solution are expressed in eqn (5)–(9).⁵⁶



Second, the forward and reverse reaction equations for the kinetically limited formation of carbamate and bicarbonate are expressed in eqn (10)–(13):⁵⁶



In Aspen Plus, the reaction rates can be expressed as power law expressions (eqn (14)).

$$R_j = k_j^\circ T^n \exp\left(-\frac{E_j}{R}\left(\frac{1}{T} - \frac{1}{298.15}\right)\right) \prod_{i=1}^N C_i^{a_{ij}} \quad (14)$$

In the above expression, the reaction rate (R_j), pre-exponential factor (k_j°), activation energy (E_j), gas constant (R), and system temperature in kelvin (T) are used. In addition, a_i and a_{ij} are the activity of i species and reaction order of species i in reaction j respectively. The power law expressions and rate constant parameters of the carbamate and (bi)carbonate reactions in the study of Zhang and Chen⁵⁷ are summarized in Table S2 in the ESI.† The gas product stream of the two CCU processes is a mixture of CO and H_2 , and are separated using PSA technology to obtain pure CO gas as a targeted product. PSA is used to separate target gas species based on the molecular characteristics of the species and the affinity for the adsorbent material by dynamically applying pressure. The PSA process involves pressurization, adsorption, depressurization, and desorption steps. In this study, a shortcut PSA model was developed as a simplified version of the dynamic model using Aspen Custom Modeler,⁵⁸ and a mathematical model for each PSA step was developed based on the assumption of ideal adsorption and desorption conditions. The Langmuir-Freundlich isotherm model (eqn (15)) was used to predict the equilibrium amount of the adsorption of gas components to the adsorbent.

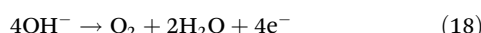
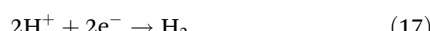
$$q = \frac{q_m (BP)^{\frac{1}{n}}}{1 + (BP)^{\frac{1}{n}}} \quad (15)$$

where q is the number of moles of adsorbed gas per unit adsorbent and P is the operating pressure, and the isotherm parameters expressed in terms of temperature include saturation capacity (q_m), affinity constant (B), and exponent (n). In addition, it was assumed that the PSA column consisted of a pressure vessel, and zeolite LiX⁵⁹ was used as an adsorbent material. Additional equations required to estimate the isotherm coefficients and parameters can be found in the study of Park *et al.*⁵⁹ Typically, carbon capture plant design is reported based on the degree of CO_2 capture and CO_2 loading of lean amine and rich amine. In this study, the lean amine loading and rich amine loading in each CCU process were designed to achieve the same values of 0.13 and 0.46 mol/mol. The corresponding CO_2 loading value is reasonable compared to the optimal values (0.132 and 0.473 mol/mol) adopted by Sipöcz and Tobiesen⁶⁰ for lean amine and rich amine by designing a commercial-scale CO_2 capture plant. The key design specifications in this study for each CCU process are shown in Tables S3 and S4 in the ESI.†

In addition to the CO_2 capture process, it is essential to consider the electrochemical CO_2 reduction reaction. In the c CO_2 RR electrolyzer cell, 30 wt% MEA and 2 M KCl were used as the catholyte, and 1 M KOH was used as the anolyte.¹⁷ Each electrolyte has to be separate, and direct contact with CO_2 gas

Published on 06 September 2023. Downloaded by University of Science and Technology of China on 10/15/2024 12:40:24 PM.

with the alkaline anolyte should be prevented due to CO₂ gas loss and thus a decrease in single pass conversion (SPC). Therefore, a membrane should be introduced, and for simple simulations, a bipolar membrane that is compatible in both the CO₂RR and cCO₂RR was employed in this study (PEM and AEM are usually incompatible in the CO₂RR and cCO₂RR, respectively).^{11,14,61,62} To operate the electrolysis cell, half reactions, reduction, and oxidation reactions were applied to each cell. The cathodic cCO₂RR is the electrochemical conversion of captured CO₂ to CO (eqn (16)). Furthermore, the hydrogen evolution reaction (HER) as an undesirable side reaction that occurs competitively with CO₂ reduction in an aqueous environment is defined in the cathode (eqn (17)). The anodic reaction is based on the O₂ evolution reaction (OER) (eqn (18)).



During the CO₂RR process, liberated CO₂ is electrochemically converted to CO by cathodic reaction (eqn (19)). In addition, the HER (eqn (17)) and OER (eqn (18)) occur at the cathode and anode, respectively.



The major operating metrics of an electrolyzer include current density, cell voltage, FE, and SPC. Several operating metric assumptions were made to simulate a CO₂ electrolyzer. Table 3 shows the current and optimistic performance metric scenarios for each CO₂RR and cCO₂RR process in this study. The current conditions of the cCO₂RR were set based on Lee *et al.* to a current density of 50 mA cm⁻², 72% CO faradaic efficiency, and cell voltage of 4 V.^{14,17} In the case of CO₂RR current performance, previous studies achieved a total current density of 200 mA cm⁻² in the CO₂RR at 2.3 V⁶³ and over 300 mA cm⁻² at 2.75 V.^{15,48,64} In addition, based on the reported actual CO₂RR performances (Table 2), current density of 200 mA cm⁻², CO faradaic efficiency of 90%, and cell voltage of 3 V were assumed for the CO₂RR current conditions. In the optimistic scenario, we assumed that the cCO₂RR has the same performance as the current level of the CO₂RR. The extent to which the capture medium is regenerated in the carbon capture process can be confirmed through the lean amine CO₂ loading value. In the cCO₂RR process without a stripper unit, if the cCO₂RR electrolyzer does not achieve a

Table 3 Current and optimistic performance metric scenarios for each CO₂RR and cCO₂RR process

Scenarios		Current density (mA cm ⁻²)	Faradaic efficiency (%)	Cell voltage (V)
Current	CO ₂ RR	200	90	3
	cCO ₂ RR	50	72	4
Optimistic	CO ₂ RR	200	90	3
	cCO ₂ RR	200	90	3

sufficiently low lean amine loading of less than 0.3 mol_{CO₂} mol_{amine}⁻¹,¹⁴ this will adversely affect the CO₂ capture rate at the absorber unit. For an equivalent comparison with the CO₂RR process in which 70% of amine regeneration is performed in the stripper, the SPC of the cCO₂RR was set at 70% to have the same lean/rich amine loading values as the CO₂RR, which equalizes the overall CO₂ capture and regeneration capacity.

For the accurate thermodynamic analysis of the MEA-H₂O-CO₂ system, an electrolyte nonrandom two-liquid (ELECNRTL)^{65–67} model was used for the liquid phase activity coefficients. In addition, the PC-SAFT equation of state^{68,69} was applied for vapor phase fugacity coefficients. These models have been verified by Chen *et al.*⁷⁰ Furthermore, thermophysical property variables from Aspen Plus data bank⁷¹ (Tables S5–S17, ESI†) were applied. These properties enabled the establishment of the foundation for more reliable process modeling.

Parameters and metrics in the techno-economic analysis and life cycle assessment

Techno-economic analysis methodology. Herein, we conducted a techno-economic analysis, involving an existing subcritical pulverized coal-fired power plant⁵⁵ as an upstream process, of the cCO₂RR and CO₂RR processes. All economic evaluations and global economic assumptions (Table S18, ESI†) in this study were based on the NETL cost estimation methodology⁷² to calculate the exact cost required for the designed process. In particular, since the cCO₂RR process and the CO₂ utilization part of the CO₂RR process are new concepts with limited data processes, 40% process contingency was set according to the Association for the Advancement of Cost Engineering International (AACE) guideline.⁷² Also, in the case of the carbon capture process, 10% contingency was set because it was commercially used. The economic feasibility of the general carbon capture and storage (CCS) process was evaluated based on the CO₂ capture cost, also known as the CO₂ avoided cost. Although the current CCS process based on MEA solvents exhibit high capture costs ranging from \$44 per t_{CO₂} to \$70 per t_{CO₂},^{17,73} an enhanced economic feasibility is expected if the CCU technology is used instead of CCS. This is because the CCU technology can simultaneously captures CO₂ and produces value-added products using captured CO₂, while reducing CO₂ emissions. Therefore, to analyze the economic advantage of the CCU process over the existing commercialized carbon capture process, the capture cost of the cCO₂RR and CO₂RR was calculated and compared, while using carbon capture process as an economic index. The formula used to calculate the capture cost based on NETL's cost estimation methodology is expressed in eqn (20).⁷²

$$\text{CO}_2 \text{ capture cost} =$$

$$\frac{\{\text{COE}_{\text{with removal}} - \text{COE}_{\text{reference}}\}[\$ \text{per MW h}]}{\{\text{CO}_2 \text{ Emissions}_{\text{reference}} - \text{CO}_2 \text{ Emissions}_{\text{with removal}}\}[\text{tons per MW h}]} \quad (20)$$

Cost of electricity (COE) used in the CO₂ capture cost equation refers to the revenue (\$ per MW h) obtained in the

first year of operation of the power plant to satisfy the finance structure assumptions of the power plant. COE is mainly used to compare the economic feasibility of energy generation sources (eqn (21)).⁷²

$$\text{COE} = \frac{\left(\begin{array}{l} \text{First year} \\ \text{Capital charge} \end{array} \right) + \left(\begin{array}{l} \text{First year fixed} \\ \text{Operating costs} \end{array} \right) + \left(\begin{array}{l} \text{First year variable} \\ \text{Operating costs} \end{array} \right)}{\left(\begin{array}{l} \text{Annual net megawatt hours} \\ \text{of power generated} \end{array} \right)} \quad (21)$$

Discounted cash flow (DCF) is a method for expressing the expected future cash flows obtained from the operating activities from plant construction to the end of operation by discounting it to the present value. The sum of present values calculated through the cash flow discount method during the plant cash flow analysis period is known as the net present value (NPV). In addition, the LCOC,⁵⁸ which represents the minimum selling price without margin at which the corresponding net present value becomes zero, can be calculated. As the market selling price of the compounds is known, LCOC can be used as an index for judging the profitability of the plant.

As this study focused on the electrochemical conversion process of CO₂, the capital cost estimation method of the electrolyzer is important. As no detailed electrolyzer cost estimation guide is directly used for CO₂ reduction or carbamate reduction, PEM water electrolyzers are used as a representative model for estimating the CO₂ electrolyzer unit cost.^{73–78} Particularly, the structure of CO₂ electrolyzers is analogous to that of PEM water electrolyzers, such as the use of metal end plates with channels and components such as porous GDEs and permselective membranes; thus, it is reasonable to calculate the cost of the CO₂ electrolyzer in the same manner as that of PEM.^{79–81} Therefore, in this study, the capital costs of

CO₂ electrolyzers were estimated by utilizing a sophisticated model (ESI Note 2, ESI†) of the cost of PEM electrolysis technology for producing H₂ from water from the DOE hydrogen analysis (H₂A) project. In addition, the cost related to the break-

down and stability of the electrolyzer components was calculated as a cell compartment replacement cost of 15% of the installed capital cost and an MEA replacement cost of 5% of the stack cost specified in Table S19 in the ESI.† In addition, the maintenance cost of the electrolyzer is equivalent to 2.5% of the capital cost.

Life cycle assessment methodology. LCA is a well-established methodology for evaluating the environmental impact of a service or product over its entire life cycle, and it was standardized by the international organization for standardization (ISO) in ISO 14040/14044.⁸² In this study, the LCA was performed using Simapro software (Version 9.3, Pre-consultants, the Netherlands) and data libraries from Ecoinvent v3.8.⁸³ The LCA settings and inventories used in this study are specified in Tables S22 and S23 in the ESI.† In addition, ReCiPe 2016 (H) v1.1,⁸⁴ a life cycle impact assessment method that includes midpoint impact categories, was used. Regarding the system boundary setting (Fig. 2), most of the previous LCA studies focused on the entire CCS chain, including the power production process.^{85,86} In contrast, previous studies aimed at directly comparing the two CCS or CCU processes applied gate-to-gate system boundaries excluding power plants.^{87,88} The upstream and downstream processes and product specifications of both processes are the same when the same power

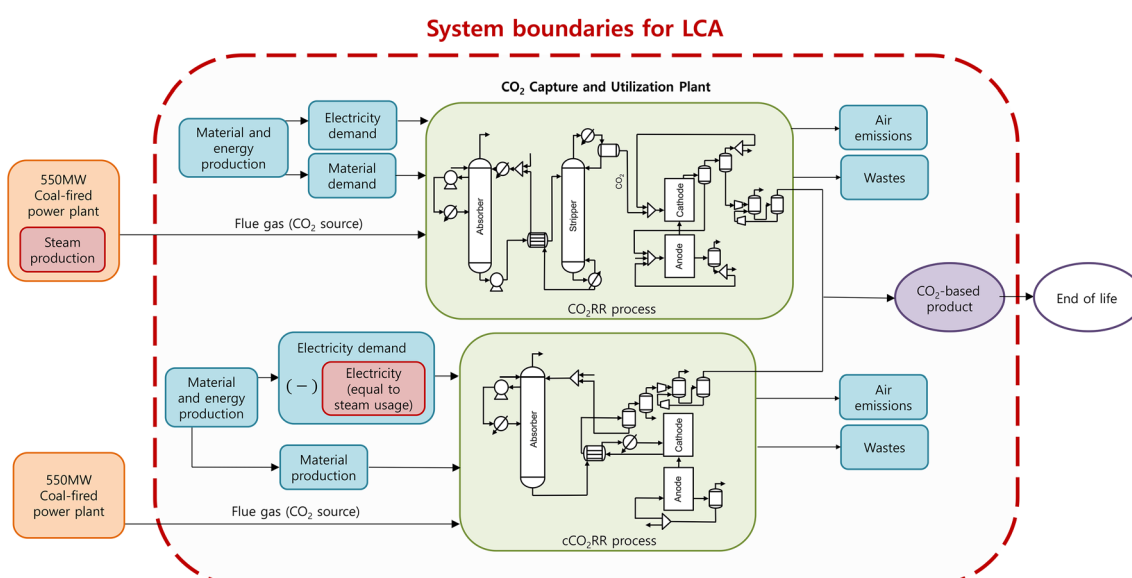


Fig. 2 System boundaries for the life cycle assessment (LCA) of cCO₂RR and CO₂RR carbon capture and utilization (CCU) processes.

plant is used as a CO₂ source. In addition, if the power production process is included in the LCA system boundary, the difference in the environmental impact between the cCO₂RR and CO₂RR processes will be inconspicuous due to the predominant impact of the fuel supply chain and the fuel combustion. Therefore, the gate-to-gate system boundary was applied to the CO₂ capture and utilization process except the power plant, and a functional unit of 1.0 kg of CO was set. Typically for post-combustion capture processes, steam is drawn and used from an upstream steam power cycle. In this study, only CCU plants excluding power plants are set as LCA boundaries, and the premise of this assumption is that each process has the same power plant with the same power generation specifications as the upstream process. In order to satisfy that assumption, LCA analysis was conducted towards reducing the electrical energy demand of the cCO₂RR process by calculating the reduction in electrical output of the power plant corresponding to the use of the regeneration heat required in the CO₂RR process. The reduction in electrical output of the power plant according to steam usage was calculated based on NETL data with a net plant efficiency (HHV) of 36.78%,⁵⁵ so the 230 000 kW of thermal energy used by the reboiler was converted to 84 597 kWe. Furthermore, in this comparative study, the environmental effects of plant construction and decommissioning processes were ignored.

Results and discussion

Determination of the economic potential based on the CO₂ capture cost

The capture cost of 1 ton of CO₂ gas is one of the major descriptors for evaluating the economic feasibility of the CCUS

technology. It is well known that the CO₂ capture cost of the relatively matured MEA-based CO₂ capture technology ranges from \$44 per t_{CO₂} to \$70 per t_{CO₂} (Fig. 3, blue shaded region) depending on the basements.^{17,73} As a reference, the CO₂ capture cost of DOE's NETL subcritical PC CCS plant is \$68 per t_{CO₂}.⁵⁵ The reference CCS plant and CO₂RR have the same capture cost of \$68 per t_{CO₂} when the CO selling price is \$1.22 per kg (Fig. 3a), whereas the current case cCO₂RR's capture cost is \$1750 per t_{CO₂} at the same CO selling price conditions (\$1.22 per kg), which is significantly high. However, under an optimistic case, the cCO₂RR shows a more positive capture cost than the CO₂RR with a capture cost of \$25 per t_{CO₂}, so the cCO₂RR has better economics than the CO₂RR when the same electrochemical performances are reached. When considering the CCU process including the CO₂ utilization step, it should be noted that the capture cost is directly affected by changes in the selling price of the CO product, which is illustrated as a linear relationship between the CO selling price and CO₂ capture cost (Fig. 3b). When the CO selling price is over \$1.1 per kg, the cCO₂RR process in the optimistic case is in the competitive capture cost range. The recent CO selling price is approximately \$0.8 per kg,⁸⁹ but the CO price of \$1.1 per kg represents considerable economic feasibility because CO price is highly volatile with oil prices and has a possibility of increasing.^{90,91} Furthermore, the CO₂ capture cost of the cCO₂RR even can be zero when the CO selling price is greater than \$1.25 per kg. In terms of the cCO₂RR, the main driver of lower capture cost is process intensification, and capture cost analysis revealed that the CCU technology can have a sufficiently economic advantage over the CCS depending on the CO selling price. In fact, the cCO₂RR has low economic feasibility in the current case due to the low level of current technology. However, the cCO₂RR can be an effective alterna-

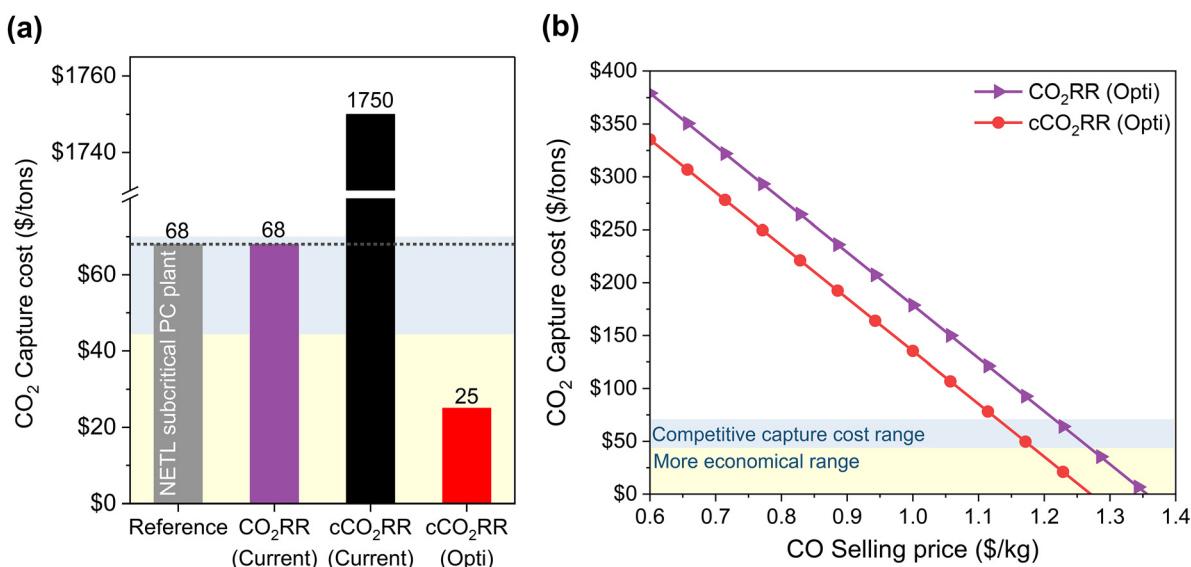


Fig. 3 Comparison of the CO₂ capture costs of CO₂RR and cCO₂RR with reference to the CCS capture cost based on MEA solvent (\$68 per t_{CO₂})⁵⁵ in different scenarios. (a) CO₂ capture costs at a CO selling price of \$1.22 per kg. (b) CO₂ capture costs versus CO product selling price in optimistic scenario.

tive to the conventional petroleum-based CO production system if it grows only to the level of technology of the CO₂RR as in the optimistic case.

Comparative study between cCO₂RR and CO₂RR process

For a better comparison of the economic feasibility of the cCO₂RR and CO₂RR, we analyzed the capital cost (capex) and operating cost (opex) per unit processes (Fig. 4a and b). At the current case of the electrolyzer performances, due to the low performance of the cCO₂RR, the capex of the electrolysis section is 4.8 times higher than that of the corresponding section of the CO₂RR, and the opex used for electrolysis is 2.1 times higher. However, in the optimistic case assuming that the electrochemical performances of the two processes are the same, the capex and opex of the cCO₂RR reduced by 1.27% and 12% compared to that of the CO₂RR, respectively. There was no significant difference in the capex as both processes were dominated by the cost of commercial-scale electrolyzers. In fact, the stripper of the CO₂RR process has a high equipment cost of \$44 658 000, but it is not that large compared to the much higher price of \$2 242 288 000 for the CO₂ electrolyzer. The process intensification of the cCO₂RR resulted in a

12% reduction in the opex due to the removal of the high energy requirements of the MEA regeneration and CO₂ removal steps. The lower opex was supported by the elimination of the regeneration cost, which accounted for around 10.7% of CO₂RR's opex (Fig. S3, ESI†). In addition, the largest cost driver of the opex is the large amount of electricity for electrochemical conversion, which accounts for the majority. A detailed total capex and opex cost breakdown including contingency fee, owner's cost and fixed operating cost is shown in Fig. S4 and S5, ESI†. These results indicate that both capex and opex exhibit a sensitive correlation to the electrochemical performances of the electrolyzer. The effect of electrochemical performances, such as FE, current density, and overpotential, on the total cost are important for the development of the future performance metrics of cCO₂RR.

As current density is inversely proportional to the electrode area, a high current density can ensure a significant reduction in the capex by reducing the scale of the electrolyzer. With an increase in the current density from 50 (current case) to 1000 mA cm⁻², the total capex of cCO₂RR (current) decreased significantly from \$48 552 MM to \$5623 MM (Fig. S4, ESI†) reducing the LCOC from \$5.67 per kg to \$0.94 per kg (Fig. 4c).

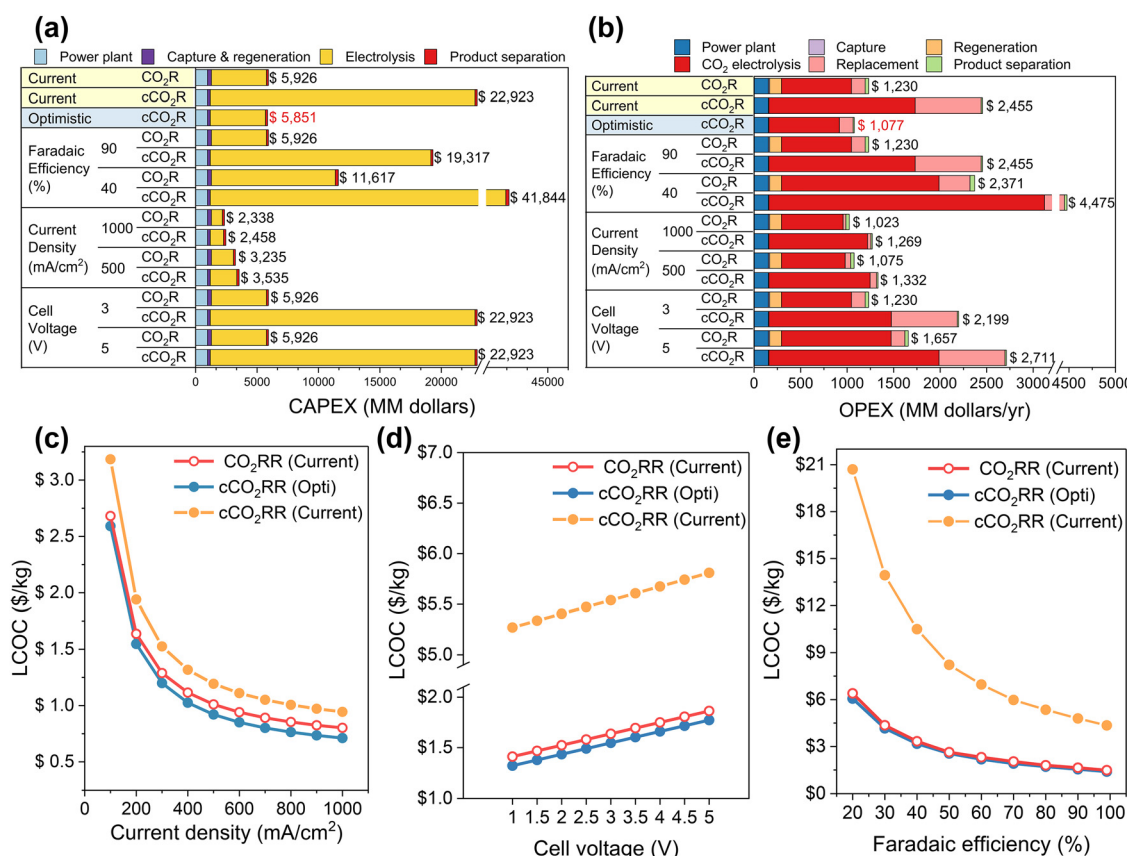


Fig. 4 Comparison of the (a) capital cost (CAPEX) and (b) operating cost (OPEX) breakdown per unit process of the cCO₂RR and CO₂RR processes under different electrochemical performance scenarios (current level, optimistic level, FE, current density, and overpotential). LCOC comparison of cCO₂RR and CO₂RR processes under different electrochemical performance scenarios according to (c) current density, (d) overpotential, (e) faradaic efficiency.

In the case of the cell voltage, as it determines the energy efficiency of CO_2 utilization, electricity consumption can be reduced with a decrease in the cell voltage, but this does not significantly affect the LCOC price (Fig. 4d). This is because the LCOC of the c CO_2 RR was predominantly determined by a capex of >70% (Fig. S6, ESI†); so capex-related parameters become more important. When considering the FE_{CO} (Fig. 4e), the LCOC of both processes decreased significantly with an increase in the FE_{CO} from 20 to 100%. FE_{CO} is a key parameter because it can affect both capex and opex. At a low FE_{CO} , the electricity consumption of the PSA process increased for the separation of pure CO gas, while simultaneously increasing the equipment cost of the electrolyzer.

These analyses indicate that a high FE_{CO} CCU system is required for a more efficient separation process and lower power consumption. This was further confirmed by the results of the sensitivity analysis (Fig. 5a), which analyzed the sensitivity of NPV when the catalyst performance and economic factors were deviated under optimistic and pessimistic performance conditions. The detailed parameters used in the sensitivity analysis are presented in Table 4. Among the electrolyzer performance parameters, the NPV of the c CO_2 RR was

Table 4 Summary of parameters and values for sensitivity analysis in different scenarios

	Pessimistic	Current	Optimistic
Electricity price (\$ kW per h)	0.07	0.05	0.03
Electrolyzer cost (\$ kW per h) ^{94,95}	460	233	130
Faradaic efficiency (%)	25	72	90
Current density (mA cm^{-2})	25	50	200
Cell potential (V)	5	4	3

highly dependent on the FE_{CO} , current density, and electrolyzer cost.

Therefore, to determine the target values of the electrolyzer catalytic performances, the contour curves representing the LCOC as a function of the FE_{CO} and current density were plotted for the c CO_2 RR and CO $_2$ RR to obtain zero NPV (Fig. 5c and d). The white and red dashed lines represent the current CO market price at \$0.8 per kg (ref. 89) and the competitive range of \$1.0 per kg,⁹² respectively, considering the price increase of petroleum-based chemicals following future oil price increase.^{90,91} The electrolyzer performances must be located above these lines for the c CO_2 RR and CO $_2$ RR to

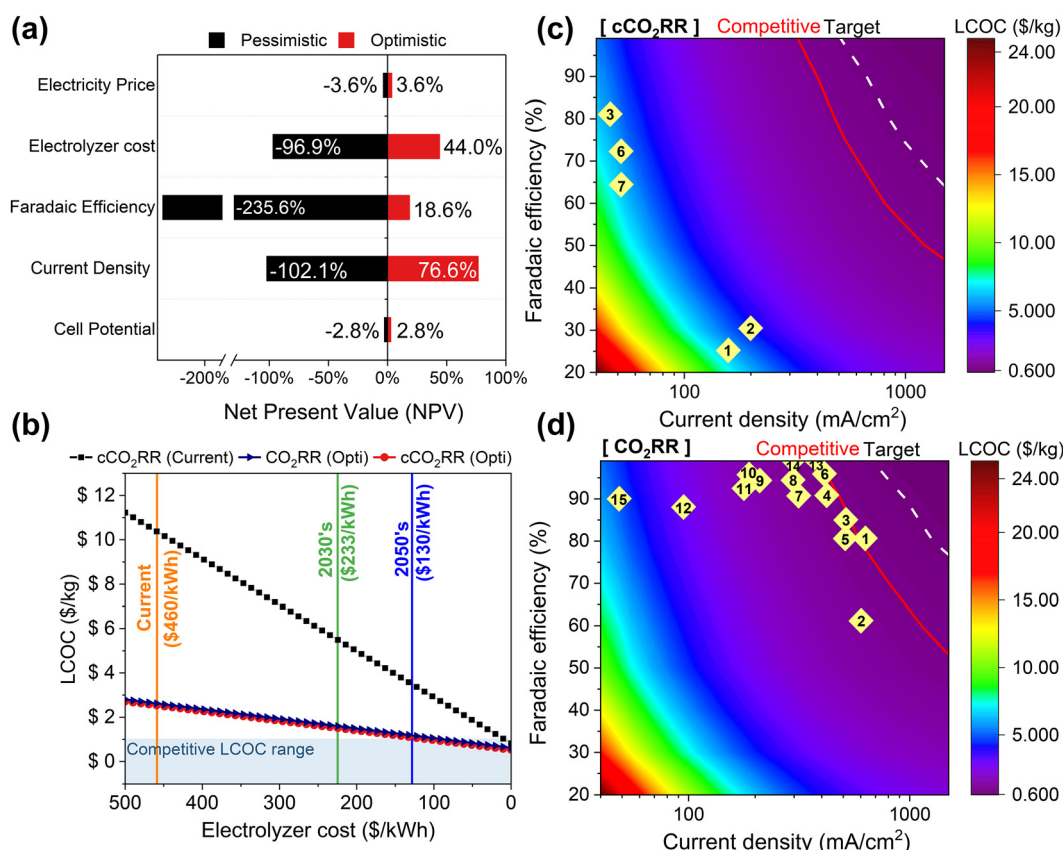


Fig. 5 (a) Net present value (NPV) deviation of the c CO_2 RR under optimistic and pessimistic performance conditions. Parameters are summarized in Table 4. (b) Comparison of the leveled cost of product CO (LCOC) of the c CO_2 RR and CO $_2$ RR processes according to electrolyzer cost under different electrochemical performances scenarios. (c and d) Electrolyzer performance contour plot showing the dependence of LCOC on FE and current density of each c CO_2 RR and CO $_2$ RR. Points depicts the current performances of each process and the number of each point means the list number of the table (c: c CO_2 RR – Table 1, d: CO $_2$ RR – Table 2).

achieve economic viability compared to petroleum-based CO products. Among the previously reported actual performances of the cCO₂RR (Table 1) and CO₂RR (Table 2), the experimental data where both FE_{CO} and current density are specified are indicated by points on the plot corresponding to each process. As a result, the CO₂RR process has a high level of technology to reach the competitive economic range, but the current technology level is insufficient for the cCO₂RR process to have economic feasibility, and the development of electrochemical performance is essential. Based on the highest FE_{CO} value (81%) among previously reported actual cCO₂RR performances,^{4,11,17,20,38–40} a current density of 900 mA cm⁻² is required to achieve the target economic range (\$0.8 per kg). However, considering the competitive range of CO prices (\$1.0 per kg), a current density of 510 mA cm⁻² is required. Recent cCO₂RR performances are significantly lower than the target range. Nevertheless, the cCO₂RR is an emerging technology; therefore its catalytic performances can be improved by designing capturing materials, catalysts, and cell configurations (further details on this are discussed in the challenges and opportunity section).

In fact, as there is a limit to the enhancement in the catalytic performance, to commercialize the cCO₂RR process in the future, it is necessary to consider reducing the scale of the cCO₂RR system by improving the electrolyzer performances or decreasing the electrolyzer costs for units. As mentioned in the previous section, electrolyzers are currently not used on a commercial-scale,⁹³ so the current high electrolyzer price accounts for a high percentage of capex. However, the electrolyzer costs can be reduced by up to 72% (e.g., \$233 per kW h in 2030⁹⁴ and \$130 per kW h in 2050⁹⁵) through electrolyzer cost reduction strategies, such as electrolyzer construction and design, facility size increase, considering economies of scale, replacement of scarce materials, flexibility and efficiency in operations, and durability enhancement.⁹⁵ Accordingly, in this step, the effect of cost reduction of electrolyzer on the economics of the cCO₂RR and CO₂RR processes was analyzed for a more realistic cost estimation (Fig. 5b). As the electrolyzer cost is reduced from \$460 per kW h to \$130 per kW h, the LCOC of the cCO₂RR at the current case can be reduced by 66% to \$3.5 per kg. Also, the cCO₂RR process under optimal conditions has an LCOC of \$2.54 per kg at the current level electrolyzer cost (\$460 per kW h), and this value decreases to \$1.54 per kg when the electrolyzer cost is \$233 per kW h in 2030. Furthermore, with a decrease in the cost of electrolyzer to \$130 per kW h in 2050, the LCOC would achieve competitive range of CO prices (\$1.0 per kg), increasing the economic viability of cCO₂RR. The analysis of the target catalytic performance while considering the electrolyzer cost in 2050 (\$130 per kW h) revealed that 81% of FE_{CO} and 500 mA cm⁻² are required to achieve the target value range (\$0.8 per kg), and only 290 mA cm⁻² is required for the competitive value range (\$1.0 per kg). The techno-economic analysis revealed that the possibility of commercialization of cCO₂RR is expected to increase in the future if the technological level of the electrolyzer cost and catalytic performance are simultaneously improved.

Life cycle assessment for environmental effects of cCO₂RR

The techno-economic analysis revealed that the cCO₂RR process is more economically feasible than the CO₂RR process under the same electrolysis performance conditions. However, in addition to the economic perspective, the environmental impacts of both the cCO₂RR and CO₂RR are also important as the CCU technology is an additional step for reducing the negative environmental impacts of the existing process. Therefore, the environmental impacts of both processes on global warming impact (GWI), freshwater, marine, and terrestrial ecosystem, fossil resource scarcity (FRS), and humans when a functional unit of 1 kg of CO is produced through the cCO₂RR and CO₂RR were simulated using LCA (Fig. 6). The detailed environmental impact assessment results for each CCU process are tabulated in Tables S24–S29 in the ESI.† To compare the environmental impacts, the relative environmental impacts of the cCO₂RR under current and optimistic conditions were depicted by setting the environmental impacts of CO₂RR to 100%. The results revealed that compared to the CO₂RR, the negative environmental impacts of the cCO₂RR (current case) increased by 127.1% in the global warming category and up to 128.8% in the fossil resource scarcity category under the base conditions of using coal gas as an electricity source (Fig. 6a). This is caused by the high electrical energy demand due to the current low performance level of the cCO₂RR. On the other hand, in the cCO₂RR (optimistic case), the global warming impact is reduced by 4.3% and the fossil resource scarcity by 4.2% compared to the CO₂RR, respectively. Additionally, if renewable sources are used instead of fossil fuel such as coal, the GWI in the cCO₂RR (current) can be further reduced by up to 95% if hydro power is used as the power source, and the use of a variety of renewable electricity sources can reduce all environmental impact categories, including GWI (Fig. 6b). For a more precise comparison, the GWI, which is the major reason for the CCU technology, was simulated based on the emission of greenhouse gas (GHG) (Fig. 6c). The inventory of CO₂ feedstock was considered as a negative value because both processes produce CO by consuming captured CO₂. It is noteworthy that the CCU technology inevitably produces GHG as direct emission during the CCU plant operation and as indirect emission through the electricity generation and supplementation. Although the direct emission of GHG by both processes was similar, the indirect emission of GHG in the CO₂RR was larger than that in the cCO₂RR (optimistic case). This is due to the steam supply for the regeneration of capture CO₂ in the CO₂RR, and as mentioned in the life cycle assessment methodology section above, the effect of steam usage is expressed as a reduction in electrical energy demand in the cCO₂RR process. Among the indirect emissions, electricity generation was the largest contributor to the total GWI. In particular, among the impacts of electricity generation analyzed through GWI breakdown result of impacts in terms of unit process (capture, electrolysis, product separation), the electrochemical conversion section accounts for more than 90%, which was attributed to the fact that coal gas

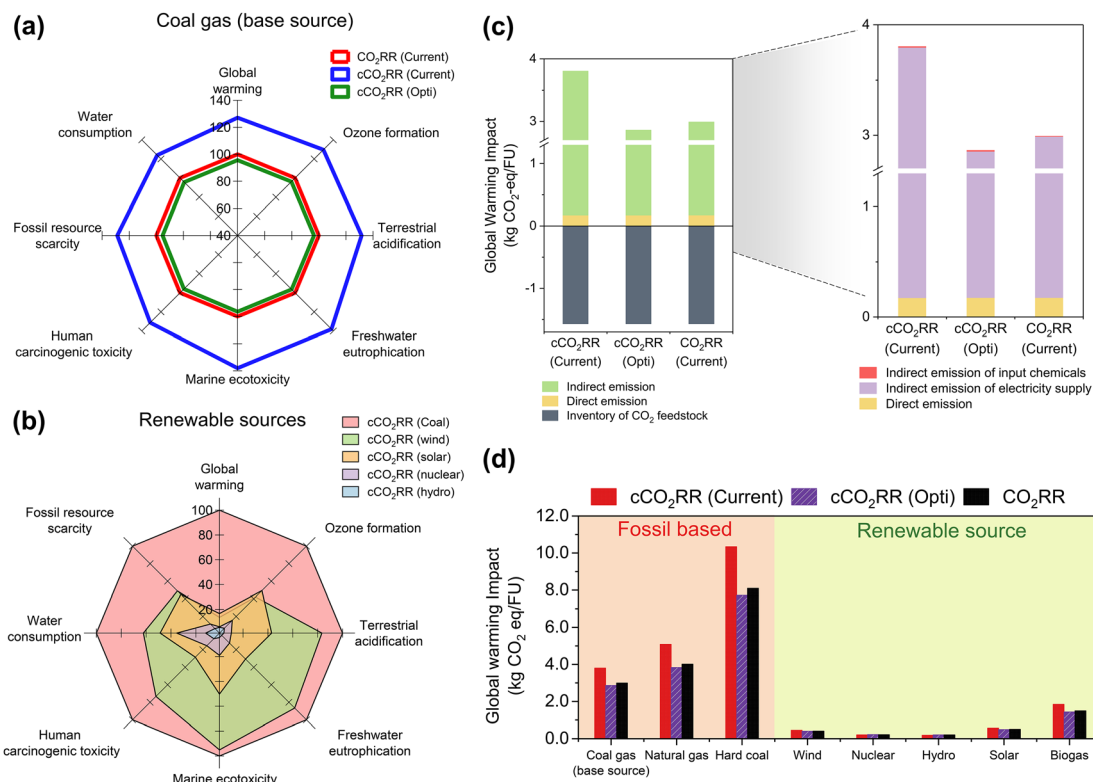


Fig. 6 Comparison of the environmental relative contributions of the cCO₂RR and CO₂RR processes under different electrochemical performance scenarios (current level, optimistic level) according to various electricity sources: (a) coal gas source as the base case and (b) renewable sources. Comparison of the global warming impact (GWI) according to: (c) component contribution and (d) various sources.

is the base case electricity source (Fig. S7, ESI†). Accordingly, changing the electricity source in the cCO₂RR process to a renewable source can further reduce the GWI (Fig. 6d), and even the GWI of cCO₂RR (current) can be lower than CO₂RR because the impact from electricity consumption is clearly reduced.

Shifting toward low-carbon electricity source is an essential element of climate change mitigation strategies and electrochemical processes. This is because various feedstocks and technologies used to generate electricity have different environmental impacts. Therefore, we investigated the environmental impacts of eight different sources of electricity (1) coal gas (base case); (2) natural gas; (3) hard coal; (4) wind power; (5) nuclear power; (6) hydro power; (7) concentrating solar power; and (8) biogas on the GWI (kg CO₂ eq.) (Table S30, ESI†). The results revealed that the use of a hydro power source in the cCO₂RR can reduce the GWI index by approximately 95% (current) and 93% (optimistic) compared to coal gas. In the case of the CO₂RR, the GWI decreased by 93%. Accordingly, nuclear and hydro powers exerted the most positive environmental impact on the cCO₂RR. In summary, in the current case of the cCO₂RR, it has a more adverse effect on the environment than the CO₂RR due to the large amount of electricity consumed due to its low performance, but if a renewable energy source such as nuclear power or hydropower is used as the electricity source, it can be an environmentally

friendly process than CO₂RR by showing a lower GWI (about 0.2 kg CO₂ eq.).

Challenges and opportunities

Improvements in cCO₂RR performances. The techno-economic analysis of the cCO₂RR performed in this study revealed that the NPV is highly dependent on the scale of the electrolyzer. To save electrolyzer cost, a high current density and high FE of the cCO₂RR, as well as a low unit price of the electrolyzer, are required to decrease the scale of the electrolyzer and achieve lower unit costs. One of the most urgent issues to achieve higher cCO₂RR performances is the understanding of the mechanism of whether the CO₂ is regenerated from carbamates before cCO₂RR²⁰ or the carbamates are directly reduced.^{17,36} Several researchers have reported that the kinetics of carbamates is independent of the concentration of carbamates but is rather governed by the cell temperature and other operation condition such as cell configuration and electrolyte composition. The results of this study indicated the regenerated CO₂ is the CO₂ source for cCO₂RR, and not a direct reduction of carbamates. However, it was proposed that the small-sized cations can assist electron transfer to carbamate by narrowing the electrochemical double layer with negatively charged carbamate. Depending on the cCO₂RR mechanism, the designing strategies for efficient cCO₂RR can be significantly changed. In this paper, we will suggest several per-

spectives on cCO₂RR based on the ambiguity of the cCO₂RR mechanism that should be considered in the future.

As cCO₂RR is an integrated CO₂ capturing and utilization technology, both the capture and electrochemical reduction of CO₂ should be simultaneously developed. In CO₂ capture, the designing of capturing materials, which provide an optimal CO₂ binding strength to promote cCO₂RR kinetics, is required. The C–N bonding energy in carbamates is determined by the nucleophilicity and bulkiness of the R-group design of amine-based capturing materials, but the relationship between C–N bonding and cCO₂RR kinetics is rarely investigated. Therefore, experimental and theoretical surveys on the various capturing materials to clarify the tradeoff between CO₂ capture, regeneration, and reduction are required. Particularly, the electron transfer to carbamates is highly dependent on the interface between the catalyst surface and electrolyte, which is sensitively modified by the bulkiness of carbamates.^{17,20,96} Less bulky amines provide narrower interfaces that facilitate electron transfer from the electrode to carbamates.^{20,36} Moreover, the viscosity, hydrophobicity, and distribution of carbamates and (bi)carbonates should be considered depending on the design of amine-based capturing materials.

In terms of CO₂ reduction, the cCO₂RR shares common concepts with catalysis: more active, selective, and larger number of reaction sites results in higher catalytic performances. Nanostructured catalysts can provide not only a larger number of active sites⁴ but also higher surface energy and different mass diffusion properties for effective CO₂RR.^{97,98} In the cCO₂RR, however, the surface charge of catalysts can be confined by the bulkiness of carbamates and ammonium compared to CO₂RR.¹⁷ SACs with a single atomic active center have demonstrated higher cCO₂RR performances compared to noble-metal catalysts because of less sterically hindered surficial conditions.²⁰ Therefore, the tailoring of the morphologies of SACs can be a feasible strategy to obtain a larger number of active sites without the steric hindrance of bulky carbamates and ammonium in the electrochemical double layer.

The performances of the cCO₂RR are also sensitively modified by the microenvironments near the catalyst surfaces through the catalyst design and cell configuration. Membrane electrode assembly configurations with no gaps between electrodes and membrane have demonstrated higher cCO₂RR performances by reducing ohmic losses, as well as providing protons to the catalyst layer through PEM or BPM from the anode.^{20,39} Acidic anolytes can facilitate the proton crossover to the catalyst layer, which weakens the C–N bonding in carbamates and promotes CO₂ regeneration, but low pH conditions also provide faster hydrogen evolution reaction (HER) kinetics, thus reducing the FE of the cCO₂RR.^{44,99,100} In addition, the presence of an add-on layer on the catalyst surface to buffer the acidic atmosphere can weaken the C–N bonding without promoting the HER.¹⁰¹

CO₂ conversion. The ability of the AEM electrode assembly configuration with a gas diffusion layer for significantly improving the CO₂RR by reducing ohmic losses and mitigating the mass transport limitation of CO₂ gas has been demon-

strated. However, this configuration exhibits a drawback: the CO₂ SPC to CO of this configuration is theoretically limited to 50% by the carbonate crossover from the cathode to the anode through AEM.¹⁰² As carbonates regenerate to CO₂ at the anode by oxidation, the re-capture of unreacted CO₂ occupies a huge portion of the CO₂RR cost.^{62,103} Hence, the SPC has recently emerged as a critical factor for evaluation of CO₂RR performances. In the cCO₂RR, the SPC can reach 100% in theory, compared to that in the CO₂RR,^{17,103} as the regenerated CO₂ from carbamates or carbamates themselves are reduced into CO. In this paper, however, the SPC of the cCO₂RR relied on the assumptions even though it is highly correlated to both CO₂ capture and the cCO₂RR because the CO₂ loading in the lean amine after the cCO₂RR has rarely been reported to date. Therefore, it is essential to investigate the background of the SPC of cCO₂RR to provide more precise techno-economic perspectives on the cCO₂RR in the future.

Conclusion

In this study, we reported that the direct electrochemical conversion process *via* the cCO₂RR has the potential to be an effective alternative to the conventional petroleum-based CO₂ capture and CO production systems. In fact, the cCO₂RR has low economic feasibility because of the low level of the current technology. However, if the cCO₂RR technology grows to the performance level of the CO₂RR technology, 12% lower operating cost and 6.1% lower LLOC compared to the CO₂RR can be achieved due to process intensification. In addition, for the future commercialization of the cCO₂RR process, it is essential to reduce the electrolyzer unit cost and the scale of the cCO₂RR system by improving the FE and current density of cCO₂RR because the NPV is highly dependent on the scale of the electrolyzer. Hence, the design of capturing materials and catalysts with consideration of the tradeoff among CO₂ capture, regeneration, and reduction is necessary to achieve the proposed performance level (FE_{CO} = 81% and current density = 500 mA cm⁻²) with a comparable LLOC to that of conventional CO production. Furthermore, considering environmental aspects based on LCA, when renewable electricity is used, the cCO₂RR process exhibits significantly positive environmental impact than the CO₂RR even at the current level of technology, which will be the basis for a carbon-neutral society.

Conflicts of interest

The authors have no competing interests to declare.

Author contributions

W. C., Y. J. H., and J. N. generalized the electrochemical conversion process with the captured CO₂ concept. S. L., S. P., and J. N. developed the techno-economic analysis and life-cycle

assessment platform and process simulations. S. L. performed sensitivity analysis. W. C. and J. H. K. investigated the electrochemical properties of captured CO₂ conversion. J. N. conceived and supervised the project. S. L., W. C., Y. J. H., and J. N. wrote and edited the paper. All authors discussed and commented on the manuscript.

Acknowledgements

This work was supported by a National Research Foundation of Korea (NRF) grant funded by the Korean government (2021R1A4A3025742 and RS-2023-00259920).

References

- 1 A. Kätelhön, *et al.*, Climate change mitigation potential of carbon capture and utilization in the chemical industry, *Proc. Natl. Acad. Sci. U. S. A.*, 2019, **116**(23), 11187–11194.
- 2 I. Sullivan, *et al.*, Coupling electrochemical CO₂ conversion with CO₂ capture, *Nat. Catal.*, 2021, **4**(11), 952–958.
- 3 S. Chen, *et al.*, A critical review on deployment planning and risk analysis of carbon capture, utilization, and storage (CCUS) toward carbon neutrality, *Renewable Sustainable Energy Rev.*, 2022, **167**, 112537.
- 4 L. Chen, *et al.*, Electrochemical reduction of carbon dioxide in a monoethanolamine capture medium, *ChemSusChem*, 2017, **10**(20), 4109–4118.
- 5 O. Khalifa, *et al.*, Modifying absorption process configurations to improve their performance for Post-Combustion CO₂ capture—What have we learned and what is still Missing?, *Chem. Eng. J.*, 2022, **430**, 133096.
- 6 B. Zhao, *et al.*, Enhancing the energetic efficiency of MDEA/PZ-based CO₂ capture technology for a 650 MW power plant: Process improvement, *Appl. Energy*, 2017, **185**, 362–375.
- 7 U. Lee, *et al.*, Techno-economic optimization of a green-field post-combustion CO₂ capture process using superstructure and rate-based models, *Ind. Eng. Chem. Res.*, 2016, **55**(46), 12014–12026.
- 8 F. A. Chowdhury, *et al.*, Synthesis and selection of hindered new amine absorbents for CO₂ capture, *Energy Procedia*, 2011, **4**, 201–208.
- 9 F. A. Chowdhury, *et al.*, CO₂ capture by tertiary amine absorbents: a performance comparison study, *Ind. Eng. Chem. Res.*, 2013, **52**(24), 8323–8331.
- 10 S. A. Freeman, *et al.*, Carbon dioxide capture with concentrated, aqueous piperazine, *Int. J. Greenhouse Gas Control*, 2010, **4**(2), 119–124.
- 11 K. M. G. Langie, *et al.*, Toward economical application of carbon capture and utilization technology with near-zero carbon emission, *Nat. Commun.*, 2022, **13**(1), 7482.
- 12 D. Bahamon, *et al.*, A comparative assessment of emerging solvents and adsorbents for mitigating CO₂ emissions from the industrial sector by using molecular modeling tools, *Front. Energy Res.*, 2020, **8**, 165.
- 13 A. Al-Mamoori, *et al.*, Carbon capture and utilization update, *Energy Technol.*, 2017, **5**(6), 834–849.
- 14 M. Li, *et al.*, Energy comparison of sequential and integrated CO₂ capture and electrochemical conversion, *Nat. Commun.*, 2022, **13**(1), 5398.
- 15 D. Kim, *et al.*, Electrocatalytic reduction of low concentrations of CO₂ gas in a membrane electrode assembly electrolyzer, *ACS Energy Lett.*, 2021, **6**(10), 3488–3495.
- 16 B.-U. Choi, *et al.*, System design considerations for enhancing electroproduction of formate from simulated flue gas, *ACS Sustainable Chem. Eng.*, 2021, **9**(5), 2348–2357.
- 17 G. Lee, *et al.*, Electrochemical upgrade of CO₂ from amine capture solution, *Nat. Energy*, 2021, **6**(1), 46–53.
- 18 C. M. Jens, *et al.*, To integrate or not to integrate—techno-economic and life cycle assessment of CO₂ capture and conversion to methyl formate using methanol, *ACS Sustainable Chem. Eng.*, 2019, **7**(14), 12270–12280.
- 19 E. Pérez-Gallent, *et al.*, Integrating CO₂ capture with electrochemical conversion using amine-based capture solvents as electrolytes, *Ind. Eng. Chem. Res.*, 2021, **60**(11), 4269–4278.
- 20 J. H. Kim, *et al.*, Insensitive cation effect on single-atom Ni catalyst allows selective electrochemical conversion of captured CO₂ in universal media, *Energy Environ. Sci.*, 2022, **15**(10), 4301–4312.
- 21 J. W. Maina, *et al.*, Strategies for integrated capture and conversion of CO₂ from dilute flue gases and the atmosphere, *ChemSusChem*, 2021, **14**(8), 1805–1820.
- 22 J. Kothandaraman, *et al.*, CO₂ capture by amines in aqueous media and its subsequent conversion to formate with reusable ruthenium and iron catalysts, *Green Chem.*, 2016, **18**(21), 5831–5838.
- 23 S. Kar, *et al.*, Advances in catalytic homogeneous hydrogenation of carbon dioxide to methanol, *J. CO₂ Util.*, 2018, **23**, 212–218.
- 24 D. A. Jones, *Technoeconomic Evaluation of MEA versus Mixed Amines and a Catalyst System for CO₂ Removal at Near-Commercial Scale at Duke Energy Gibson 3 Plant and Duke Energy Buck NGCC Plant*, Lawrence Livermore National Lab. (LLNL), Livermore, CA, United States, 2018.
- 25 J. Sun, *et al.*, High Throughput Preparation of Ag-Zn Alloy Thin Films for the Electrocatalytic Reduction of CO₂ to CO, *Materials*, 2022, **15**(19), 6892.
- 26 K. Williams, *et al.*, Protecting effect of mass transport during electrochemical reduction of oxygenated carbon dioxide feedstocks, *Sustainable Energy Fuels*, 2019, **3**(5), 1225–1232.
- 27 S. E. Jerng and B. M. Gallant, Electrochemical Reduction of CO₂ in the Captured State using Aqueous or Non-aqueous Amines, *iScience*, 2022, 104558.
- 28 C. Wu, T. P. Senftle and W. F. Schneider, First-principles-guided design of ionic liquids for CO₂ capture, *Phys. Chem. Chem. Phys.*, 2012, **14**(38), 13163–13170.

- 29 P. Mores, N. Scenna and S. Mussati, CO₂ capture using monoethanolamine (MEA) aqueous solution: Modeling and optimization of the solvent regeneration and CO₂ desorption process, *Energy*, 2012, **45**(1), 1042–1058.
- 30 G. Pellegrini, R. Strube and G. Manfrida, Comparative study of chemical absorbents in postcombustion CO₂ capture, *Energy*, 2010, **35**(2), 851–857.
- 31 R. Sharifian, *et al.*, Electrochemical carbon dioxide capture to close the carbon cycle, *Energy Environ. Sci.*, 2021, **14**(2), 781–814.
- 32 S. Y. W. Chai, L. H. Ngu and B. S. How, Review of carbon capture absorbents for CO₂ utilization, *Greenhouse Gases: Sci. Technol.*, 2022, **12**(3), 394–427.
- 33 G. Wang, J. Pan and H. Yang, Gas phase electrochemical conversion of humidified CO₂ to CO and H₂ on proton-exchange and alkaline anion-exchange membrane fuel cell reactors, *J. CO₂ Util.*, 2018, **23**, 152–158.
- 34 J. J. Kaczur, *et al.*, Carbon dioxide and water electrolysis using new alkaline stable anion membranes, *Front. Chem.*, 2018, **6**, 263.
- 35 C. M. Gabardo, *et al.*, Continuous carbon dioxide electro-reduction to concentrated multi-carbon products using a membrane electrode assembly, *Joule*, 2019, **3**(11), 2777–2791.
- 36 A. Khurram, *et al.*, Promoting amine-activated electrochemical CO₂ conversion with alkali salts, *J. Phys. Chem. C*, 2019, **123**(30), 18222–18231.
- 37 S. Hernández, *et al.*, Syngas production from electrochemical reduction of CO₂: current status and prospective implementation, *Green Chem.*, 2017, **19**(10), 2326–2346.
- 38 Y. C. Li, *et al.*, CO₂ electroreduction from carbonate electrolyte, *ACS Energy Lett.*, 2019, **4**(6), 1427–1431.
- 39 T. Li, *et al.*, Electrolytic conversion of bicarbonate into CO in a flow cell, *Joule*, 2019, **3**(6), 1487–1497.
- 40 T. Li, *et al.*, Conversion of bicarbonate to formate in an electrochemical flow reactor, *ACS Energy Lett.*, 2020, **5**(8), 2624–2630.
- 41 E. W. Lees, *et al.*, Electrolytic methane production from reactive carbon solutions, *ACS Energy Lett.*, 2022, **7**(5), 1712–1718.
- 42 B. Endrődi, *et al.*, High carbonate ion conductance of a robust PiperION membrane allows industrial current density and conversion in a zero-gap carbon dioxide electrolyzer cell, *Energy Environ. Sci.*, 2020, **13**(11), 4098–4105.
- 43 S. H. Yang, *et al.*, Membrane Engineering Reveals Descriptors of CO₂ Electroreduction in an Electrolyzer, *ACS Energy Lett.*, 2023, **8**(4), 1976–1984.
- 44 Z. Yin, *et al.*, An alkaline polymer electrolyte CO₂ electrolyzer operated with pure water, *Energy Environ. Sci.*, 2019, **12**(8), 2455–2462.
- 45 B. Endrődi, *et al.*, Operando cathode activation with alkali metal cations for high current density operation of water-fed zero-gap carbon dioxide electrolyzers, *Nat. Energy*, 2021, **6**(4), 439–448.
- 46 K. Ye, *et al.*, Resolving local reaction environment toward an optimized CO₂-to-CO conversion performance, *Energy Environ. Sci.*, 2022, **15**(2), 749–759.
- 47 R. Wang, *et al.*, Maximizing Ag utilization in high-rate CO₂ electrochemical reduction with a coordination polymer-mediated gas diffusion electrode, *ACS Energy Lett.*, 2019, **4**(8), 2024–2031.
- 48 W. H. Lee, *et al.*, Highly selective and scalable CO₂ to CO-Electrolysis using coral-nanostructured Ag catalysts in zero-gap configuration, *Nano Energy*, 2020, **76**, 105030.
- 49 B. Endrődi, *et al.*, Multilayer electrolyzer stack converts carbon dioxide to gas products at high pressure with high efficiency, *ACS Energy Lett.*, 2019, **4**(7), 1770–1777.
- 50 G. O. Larrazábal, *et al.*, Analysis of mass flows and membrane cross-over in CO₂ reduction at high current densities in an MEA-type electrolyzer, *ACS Appl. Mater. Interfaces*, 2019, **11**(44), 41281–41288.
- 51 P. Mardle, *et al.*, Carbonate Ion crossover in zero-gap, KOH anolyte CO₂ electrolysis, *J. Phys. Chem. C*, 2021, **125**(46), 25446–25454.
- 52 A. Ozden, *et al.*, Gold adparticles on silver combine low overpotential and high selectivity in electrochemical CO₂ conversion, *ACS Appl. Energy Mater.*, 2021, **4**(8), 7504–7512.
- 53 J. W. Park, *et al.*, Bimetallic Gold–Silver Nanostructures Drive Low Overpotentials for Electrochemical Carbon Dioxide Reduction, *ACS Appl. Mater. Interfaces*, 2022, **14**(5), 6604–6614.
- 54 H.-Y. Jeong, *et al.*, Achieving highly efficient CO₂ to CO electroreduction exceeding 300 mA cm⁻² with single-atom nickel electrocatalysts, *J. Mater. Chem. A*, 2019, **7**(17), 10651–10661.
- 55 J. Haslback, *et al.*, *Cost and Performance Baseline for Fossil Energy Plants, Volume 1: Bituminous Coal and Natural Gas to Electricity, Revision 2a*, National Energy Technology Laboratory (NETL), Pittsburgh, PA, Morgantown, WV, 2013.
- 56 E. Agbonghae, *et al.*, Optimal process design of commercial-scale amine-based CO₂ capture plants, *Ind. Eng. Chem. Res.*, 2014, **53**(38), 14815–14829.
- 57 Y. Zhang and C.-C. Chen, Modeling CO₂ absorption and desorption by aqueous monoethanolamine solution with Aspen rate-based model, *Energy Procedia*, 2013, **37**, 1584–1596.
- 58 J. Na, *et al.*, General technoeconomic analysis for electrochemical coproduction coupling carbon dioxide reduction with organic oxidation, *Nat. Commun.*, 2019, **10**(1), 1–13.
- 59 Y. Park, *et al.*, Adsorption equilibria and kinetics of six pure gases on pelletized zeolite 13X up to 1.0 MPa: CO₂, CO, N₂, CH₄, Ar and H₂, *Chem. Eng. J.*, 2016, **292**, 348–365.
- 60 N. Sipöcz and F. A. Tobiesen, Natural gas combined cycle power plants with CO₂ capture—Opportunities to reduce cost, *Int. J. Greenhouse Gas Control*, 2012, **7**, 98–106.
- 61 K. Yang, *et al.*, Cation-driven increases of CO₂ utilization in a bipolar membrane electrode assembly for CO₂ electrolysis, *ACS Energy Lett.*, 2021, **6**(12), 4291–4298.

- 62 C. P. O'Brien, *et al.*, Single pass CO₂ conversion exceeding 85% in the electrosynthesis of mult carbon products via local CO₂ regeneration, *ACS Energy Lett.*, 2021, **6**(8), 2952–2959.
- 63 S. Ma, *et al.*, One-step electrosynthesis of ethylene and ethanol from CO₂ in an alkaline electrolyzer, *J. Power Sources*, 2016, **301**, 219–228.
- 64 S. Verma, *et al.*, The effect of electrolyte composition on the electroreduction of CO₂ to CO on Ag based gas diffusion electrodes, *Phys. Chem. Chem. Phys.*, 2016, **18**(10), 7075–7084.
- 65 Y. Song and C.-C. Chen, Symmetric electrolyte nonrandom two-liquid activity coefficient model, *Ind. Eng. Chem. Res.*, 2009, **48**(16), 7788–7797.
- 66 C. C. Chen and L. B. Evans, A local composition model for the excess Gibbs energy of aqueous electrolyte systems, *AIChE J.*, 1986, **32**(3), 444–454.
- 67 C. C. Chen, *et al.*, Local composition model for excess Gibbs energy of electrolyte systems. Part I: Single solvent, single completely dissociated electrolyte systems, *AIChE J.*, 1982, **28**(4), 588–596.
- 68 J. Gross and G. Sadowski, Perturbed-chain SAFT: An equation of state based on a perturbation theory for chain molecules, *Ind. Eng. Chem. Res.*, 2001, **40**(4), 1244–1260.
- 69 J. Gross and G. Sadowski, Application of the perturbed-chain SAFT equation of state to associating systems, *Ind. Eng. Chem. Res.*, 2002, **41**(22), 5510–5515.
- 70 Y. Zhang, H. Que and C.-C. Chen, Thermodynamic modeling for CO₂ absorption in aqueous MEA solution with electrolyte NRTL model, *Fluid Phase Equilib.*, 2011, **311**, 67–75.
- 71 A. Plus, *Aspen physical property system V7. 2*, 2010.
- 72 J. Theis, *Quality Guidelines for Energy Systems Studies: Cost Estimation Methodology for NETL Assessments of Power Plant Performance*-Feb 2021, National Energy Technology Laboratory (NETL), Pittsburgh, PA, Morgantown, WV, 2021.
- 73 M. Jouny, W. Luc and F. Jiao, General techno-economic analysis of CO₂ electrolysis systems, *Ind. Eng. Chem. Res.*, 2018, **57**(6), 2165–2177.
- 74 J. M. Spurgeon, *et al.*, Comparative Technoeconomic Analysis of Pathways for Electrochemical Reduction of CO₂ with Methanol to Produce Methyl Formate, *ACS Sustainable Chem. Eng.*, 2022, **10**(38), 12882–12894.
- 75 X. Li, *et al.*, Greenhouse gas emissions, energy efficiency, and cost of synthetic fuel production using electrochemical CO₂ conversion and the Fischer-Tropsch process, *Energy Fuels*, 2016, **30**(7), 5980–5989.
- 76 J. M. Spurgeon and B. Kumar, A comparative technoeconomic analysis of pathways for commercial electrochemical CO₂ reduction to liquid products, *Energy Environ. Sci.*, 2018, **11**(6), 1536–1551.
- 77 F. Chang, *et al.*, Technoeconomic analysis and process design for CO₂ electroreduction to CO in ionic liquid electrolyte, *ACS Sustainable Chem. Eng.*, 2021, **9**(27), 9045–9052.
- 78 Z. Huang, *et al.*, The economic outlook for converting CO₂ and electrons to molecules, *Energy Environ. Sci.*, 2021, **14**(7), 3664–3678.
- 79 H. Yang, *et al.*, CO₂ conversion to formic acid in a three compartment cell with SustainionTM membranes, *ECS Trans.*, 2017, **77**(11), 1425.
- 80 S. D. Sajjad, *et al.*, Tunable-high performance SustainionTM anion exchange membranes for electrochemical applications, *ECS Trans.*, 2017, **77**(11), 1653.
- 81 Y. J. Sa, *et al.*, Catalyst-electrolyte interface chemistry for electrochemical CO₂ reduction, *Chem. Soc. Rev.*, 2020, **49**(18), 6632–6665.
- 82 DIN, E., 14040: 2009–11 Environmental management; Life cycle assessment; Principles and framework (ISO 14040: 2006) German and English version EN ISO 14040: 2006. German Institute for Standardization, 2006.
- 83 G. Wernet, *et al.*, The ecoinvent database version 3 (part I): overview and methodology, *Int. J. Life Cycle Assess.*, 2016, **21**(9), 1218–1230.
- 84 M. A. Huijbregts, *et al.*, ReCiPe2016: a harmonised life cycle impact assessment method at midpoint and endpoint level, *Int. J. Life Cycle Assess.*, 2017, **22**(2), 138–147.
- 85 M. Rosental, T. Fröhlich and A. Liebich, Life cycle assessment of carbon capture and utilization for the production of large volume organic chemicals, *Front. Clim.*, 2020, **2**, 586199.
- 86 N. Von Der Assen, *et al.*, Life cycle assessment of CO₂ capture and utilization: a tutorial review, *Chem. Soc. Rev.*, 2014, **43**(23), 7982–7994.
- 87 T. Grant, C. Anderson and B. Hooper, Comparative life cycle assessment of potassium carbonate and monoethanolamine solvents for CO₂ capture from post combustion flue gases, *Int. J. Greenhouse Gas Control*, 2014, **28**, 35–44.
- 88 L. Giordano, D. Roizard and E. Favre, Life cycle assessment of post-combustion CO₂ capture: A comparison between membrane separation and chemical absorption processes, *Int. J. Greenhouse Gas Control*, 2018, **68**, 146–163.
- 89 H. Shin, K. U. Hansen and F. Jiao, Techno-economic assessment of low-temperature carbon dioxide electrolysis, *Nat. Sustain.*, 2021, **4**(10), 911–919.
- 90 K. Zayer Kabeh, *et al.*, Techno-economic assessment of small-scale gas to liquid technology to reduce waste flare gas in a refinery plant, *Sustain. Energy Technol. Assess.*, 2023, **55**(102955).
- 91 X. Xiuzhen, W. Zheng and M. Umair, Testing the fluctuations of oil resource price volatility: a hurdle for economic recovery, *Resour. Policy*, 2022, **79**, 102982.
- 92 E. Alper and O. Y. Orhan, CO₂ utilization: Developments in conversion processes, *Petroleum*, 2017, **3**(1), 109–126.
- 93 G. Wen, *et al.*, Continuous CO₂ electrolysis using a CO₂ exsolution-induced flow cell, *Nat. Energy*, 2022, **7**(10), 978–988.
- 94 D. Peterson, J. Vickers and D. DeSantis, *Hydrogen production cost from PEM electrolysis-2019*, DOE Hydrogen Fuel Cells Program Record, 2020, p. 19009.

- 95 E. Taibi, *et al.*, Green hydrogen cost reduction: Scaling up Electrolysers to Meet the 1.5 deg. C Climate Goal, *IRENA, Abu Dhabi*, 2020.
- 96 B. M. Gallant, Breaking down hidden barriers, *Nat. Energy*, 2021, **6**(1), 13–14.
- 97 W. Choi, *et al.*, Surface overgrowth on gold nanoparticles modulating high-energy facets for efficient electrochemical CO₂ reduction, *Nanoscale*, 2021, **13**(34), 14346–14353.
- 98 H.-E. Lee, *et al.*, Concave rhombic dodecahedral Au nanocatalyst with multiple high-index facets for CO₂ reduction, *ACS Nano*, 2015, **9**(8), 8384–8393.
- 99 L. Aeshala, R. Uppaluri and A. Verma, Effect of cationic and anionic solid polymer electrolyte on direct electrochemical reduction of gaseous CO₂ to fuel, *J. CO₂ Util.*, 2013, **3**, 49–55.
- 100 E. W. Lees, *et al.*, Gas diffusion electrodes and membranes for CO₂ reduction electrolyzers, *Nat. Rev. Mater.*, 2022, **7**(1), 55–64.
- 101 J. E. Huang, *et al.*, CO₂ electrolysis to multicarbon products in strong acid, *Science*, 2021, **372**(6546), 1074–1078.
- 102 J. A. Rabinowitz and M. W. Kanan, The future of low-temperature carbon dioxide electrolysis depends on solving one basic problem, *Nat. Commun.*, 2020, **11**(1), 1–3.
- 103 A. Ozden, *et al.*, Carbon-efficient carbon dioxide electrolyzers, *Nat. Sustain.*, 2022, 1–11.